

Technical Note

# A Test Device for Microalgal Antifouling Using Fluctuating pH Values on Conductive Paints

Norbert Kamjunke <sup>1,\*</sup> , Uwe Spohn <sup>2</sup>, Christian Morig <sup>2</sup>, Georg Wagner <sup>3</sup> and Thomas R. Neu <sup>1</sup> 

<sup>1</sup> Helmholtz-Centre for Environmental Research UFZ, Brückstraße 3a, D-39114 Magdeburg, Germany; thomas.neu@ufz.de

<sup>2</sup> Fraunhofer Institute for Mechanics of Materials IWM, Walter-Hülse-Straße 1, D-06120 Halle (Saale), Germany; uwe.spohn@imws.fraunhofer.de (U.S.); christian.morig@romonta.de (C.M.)

<sup>3</sup> NTC Nano Tech Coatings GmbH, Dirminger Straße 17, D-66636 Tholey, Germany; georg.wagner@ntcgmbh.com

\* Correspondence: norbert.kamjunke@ufz.de; Tel.: +49-391-8109434; Fax: +49-391-8109150

Received: 8 May 2020; Accepted: 2 June 2020; Published: 4 June 2020



**Abstract:** Due to the current dependence on biocidal antifouling coatings for biofouling control, there is a continuing international challenge to develop more environmentally acceptable antifouling systems. Fluctuating the pH values on paint surfaces is one of these approaches. We developed an antifouling test device to investigate algal biofilms on conductive paints by using a flume with electrochemically working test panels and subsequent confocal laser scanning microscopy (CLSM) of biofilms. By employing a pole reversal of direct current, fluctuating pH values on the paint surface were generated. As a consequence of the resulting pH stress, colonization of the paint surface by diatoms decreased substantially. The density of biofilm algae decreased with increasing pH fluctuations. However, breaks between electrochemical treatments should not exceed one hour. Overall, we established an experimental setup for testing the antifouling capabilities of electrodes based on conductive paints, which could be used for further development of these varnishes.

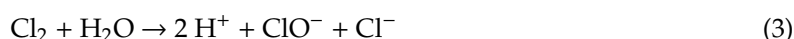
**Keywords:** antifouling; flume; conductive paint; electrochemical treatment; pH; biofilm; confocal laser scanning microscopy

## 1. Introduction

Ship hulls need to be coated with an effective antifouling system to prevent the adverse consequences of biofouling, such as the increase in energy demand for movement [1]. Organotin copolymer antifouling coatings were especially effective, but these were widely banned in 2003 following the discovery of the harmful effects of released organotins on marine and freshwater organisms [2]. Even in the absence of organotin coatings, antifouling coatings that function by the continuous release of biocides continue to be the principal method of biofouling control. This results in an ongoing challenge to develop more environmentally acceptable antifouling systems. Besides conventional antifouling paints that contain high concentrations of copper, alternative strategies, such as the imitation of natural antifouling processes, microstructured surfaces, and nonstick and fouling-release concepts, were tested [3]. In addition, superhydrophobic surfaces [4] and the removal of molecular oxygen or the addition of electron acceptor chemical species (sulfate or nitrate) [5] have been considered.

One potential approach is the application of conductive coatings that serve as electrodes for the electrolysis of sea water. Application of a current causes a pH shift on the paint surface, decreasing the pH at the positively charged anode and increasing the pH values at the negatively charged cathode.

Pairs of electrodes (see Figure 1) are pulse-wise changed from oxidizing potentials  $E_{ox}$  to reducing potentials  $E_{red}$ , and then inversely changed again. At  $E_{ox}$ , the sea water is electrochemically oxidized, accompanied mainly by the oxidation of chlorides according to Equations (1) and (2), followed by the disproportionation of chlorine Equation (3):



### Exp. 2: Electrochem. treatment

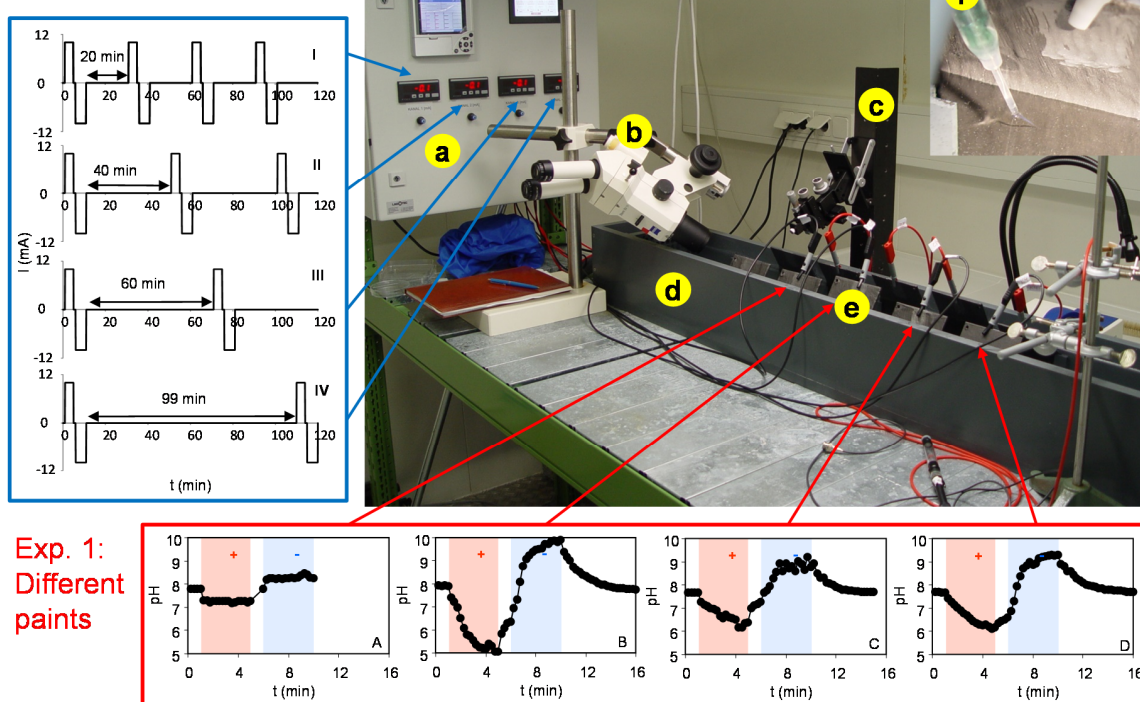


**Figure 1.** Experimental setup (photo): (a) electronic control unit with four independent ports, (b) stereo-microscope, (c) micromanipulator, (d) flume, (e) pairs of painted plates with red and black contacts and a reference pair of electrodes coated with Varnish A but without electrical contacts; insert: (f) pH probe. Experiment 1 (red frame): temporal development of pH at the surface of four paints (see Table 1 for paints A–D). Periods of positive and negative charges are marked in red and blue, respectively. Experiment 2 (blue frame): time schedule of the electrolysis current (I–IV).

**Table 1.** Properties of the used coating samples A–D. HLP: Hempel Light Primer, NTC: NanoTech Coatings, TSF: tetramethyltetraselenafulvalen, PU-G: polyurethane with graphite particles.

Varnish	Primer Layer	2nd Layer	3rd Layer
A	HLP	NTC-G45	NTC-G30
B	HLP	NTC-G45-TSF	NTC-G30
C	HLP	NTC-G45	PU-G
D	HLP	PU-G	PU-G

Concentrations of  $\text{Cl}_2$  and  $\text{ClO}^-$  are too low to have a potential toxic effect themselves. The protons are generated at or nearby the surface of the anodically working electrode. At  $E_{\text{red}}$ , water is electrochemically reduced according to Equation (4) and accompanied by the reduction of dissolved oxygen Equation (5):



Thus, the resulting excess of hydroxide ions is generated at the cathodically working electrode. Therefore, the pH nearby the cathode is drastically increased, and the pH nearby the surface of the counter electrode is decreased, in an analogous manner. Therefore, the pulse-wise changing of the electrolysis current and the periodic commutation of the electrode pairs generates a periodic and drastic change of the pH at the surface of varnished electrodes. The pH fluctuation can be increased by higher current densities during the anodic and cathodic pulses. Pole reversal results in pH fluctuation, causing severe stress for microorganisms and the larvae of higher organisms. This approach is based on German and European patents [6–8], which described the principle of the method, i.e., the pH change at the surface and the negative effect on biofouling. The method is based on graphite foil as a conductive layer, which is, however, not applicable for larger ships or too expensive. Hence, no commercial product with conductive paints is on the market as an antifouling approach so far. Moreover, the literature on electrochemical antifouling technology focuses on seawater electrolysis and the formation of chlorinated and brominated compounds [9–12]. No studies on the effect of pH change on algal biomass have been published in scientific journals to the best of our knowledge. Thus, there is the need to test conductive paints and to improve their electrochemical properties and the operational process of the electrochemical generation of pH stress. Our study describes such a test device for laboratory-scale biofouling/antifouling experiments. We developed an approach for testing selected conductive paints against microfouling under dynamic conditions in a flume. We performed a first experiment where several exemplary paints and related pH values at their surfaces were investigated with respect to their effect on algal density. In a second experiment, we aimed to find the optimal duration of the break between temporally defined impulses of the electrolysis current, which allows the suppression of biofouling at a minimum of electrochemical stress on the surface of the paint. Our test device enables a pretest as a first step to identify suitable paints, which may subsequently be tested in more detail in marine environments at a larger scale.

## 2. Materials and Methods

**Coating samples:** The paints were coated on polycarbonate panels that were 10 cm wide and 15 cm high and bent by  $30^\circ$  at the height of 10 cm. Three-layer coatings were comprised of an isolating primer layer, a second highly conductive layer guaranteeing a homogeneous distribution of the density of electrolysis current at the electrode surface, and a third conductive outer layer (Table 1). To prepare the primer, 66% (m/m) of Hempel Light Primer, 19% (m/m) of Curing Agent 95360, and 15% (m/m) of Thinner 845 were mixed for 2 min in a speed-mixer. To prepare the sol-gel NTC coatings (NanoTech Coating GmbH, Tholey, Germany), four volume parts of Et-Sil 110 marine and one volume part of Et-Sil hardener were mixed for 2 min in the speed-mixer. Proportions of 30% (m/m) and 45% (m/m) of graphite powder (synthetic, Sigma-Aldrich) were added to the stock component before mixing with the hardener to obtain NTC-G30 and NTC-G45, respectively. Both varnishes were applied by brushing five to six times, with passive curing after the third and the last brushing. NTC-G45 was used as the inner conducting layer in order to homogeneously distribute the density of the electrolysis current. The exact number of brushings did not affect electrochemical performance. For the NTC-G45-TSF-varnish, the graphite was impregnated with 89 mg tetramethyltetraselenafulvalen (TSF) in 200 mL butylacetate (BuAc). TSF was added to increase the electrical conductivity of the second layer. After the addition of another 15 mL of BuAc, the suspension was ultrasonicated for 10 min before the modified graphite was separated by filtration. The graphite modified PU-G was used to achieve a higher elasticity and an

expected higher robustness in comparison to the NTC sol–gel varnishes, which may be too recalcitrant. Varnish D was prepared to find a layering system with improved practicability. The four varnishes, A–D, listed in Table 1, were used in the first experiment, including a control without electrochemical treatment painted with Varnish A, while only Varnish A was used in the second experiment.

**Antifouling test device** (Lagotech GmbH, Magdeburg, Germany): Experiments were performed in a laboratory flume system (Figure 1). The flume had a channel length of 1.50 m, a water depth of 0.1 m, and a circulation pump for a linear flow rate of  $2 \text{ cm s}^{-1}$ , mimicking a low water flow in an inner harbor. The flume (including a storage reservoir) was filled with 60 L pure water amended with 720 g of sea salt (Tropic Marin), resulting in salinity of 12 psu, which is representative of the average salinity in Kühlungsborn at the German coast of the Baltic Sea [13]. In addition, inorganic nutrients of a diatom medium (120 mL  $\text{Ca}(\text{NO}_3)_2 \cdot 4\text{H}_2\text{O}$ , 60 mL  $\text{K}_2\text{HPO}_4$ , 150 mL  $\text{MgSO}_4 \cdot 7\text{H}_2\text{O}$ , 120 mL  $\text{Na}_2\text{CO}_3$ , 300 mL  $\text{Na}_2\text{SiO}_3 \cdot 9\text{H}_2\text{O}$ , and 300 mL micronutrient solution) were added. The electronic control unit had four independent ports for the electrochemical treatment of one pair of test panels (the coated electrodes) each. The direct current was adjusted to 10 mA at voltages between 3 and 14 mV, representing a current density of  $0.1 \text{ mA cm}^{-2}$  on the panels. The schedule for pole reversal and breaks between the current impulses was freely programmable. Figure 1 (blue frame) shows the applied time schedules I to IV of the electrolysis current: 4 min positive charge, 1 min break, 4 min negative charge, 20 min break, as described in the patent [8] for Experiment 1, and variable breaks for Experiment 2.

**pH measurement and performance of the experiment:** Pairs of painted panels were placed opposite each other in the flume and connected with the control unit, with the exception of one pair of control panels painted with the varnish A without electrochemical treatment. The pH at the paint surface was measured using a pH microprobe (pH-10, Unisense, Aarhus, Denmark) as a function of the time schedule of the electrolysis current. The microprobe was calibrated in standard buffer solutions of pH 4.0, 7.0, and 10.0. The probe was fixed at a micromanipulator and shifted as close as possible to the paint surface (see insert in Figure 1) with the help of a stereo-microscope (Stemi SV 11, Zeiss, Jena, Germany). Since diatoms are the main components of slime biofilms in marine environments [14–16], four benthic species (*Amphora coffaeiformes*, *Achnanthes brevipes*, *Nitzschia frustulum*, *Navicula salinicola*) were cultivated separately in the laboratory in diatom medium (see above) at  $21 \text{ }^\circ\text{C}$  and a light intensity of  $60 \mu\text{mol m}^{-2} \text{ s}^{-1}$  at a light–dark cycle of 12:12 h. The experiment was started directly after pH measurements. For this purpose, aliquots of about 1 L diatom culture, i.e., algal cells and diatom medium, of each species were added simultaneously to the flume as inocula. The incubation was done at a constant temperature of  $21 \text{ }^\circ\text{C}$ , and a light intensity of  $60 \mu\text{mol m}^{-2} \text{ s}^{-1}$  at a light–dark cycle of 12:12 h. The growth of diatoms was followed weekly by confocal laser scanning microscopy (see below).

**Microscopy:** The fully hydrated biofilms were examined by confocal laser scanning microscopy (Leica Microsystems, Wetzlar, Germany) for three-dimensional analysis of different cellular (chlorophyll a autofluorescence, nucleic acid stained bacteria) and polymeric biofilm constituents (glycoconjugates) [17]. The application of CLSM on painted surfaces was recently established [13,18] and showed good agreement with chlorophyll measurement [13]. Plates were disconnected from the control unit in the flow channel and transferred into Petri dishes weekly for staining. The fluor-probes were applied in the upper and lower part of the plates located at a depth of 2 and 8 cm in the circulating medium. For this purpose, two small plastic rings of 15 mm diameter and 20 mm height were glued with silicone onto the plates. The fluorescent staining was applied in this isolated ring area in order to avoid staining of the whole plate. For visualization of lectin-specific glycoconjugates in the biofilm matrix, samples were counterstained with lectin AAL (*Aleuria aurantia*) conjugated with the fluorochrome Alexa568 for 30 min at room temperature in darkness according to [19]. After rinsing with tap water three times, the samples were stained with the nucleic-acid-specific stain Syto9 for 5 min to label the bacteria. The plastic rings used for staining were removed from the plates afterwards. For CLSM, a TCS SP1 (Leica) setup with an upright microscope was available. For excitation, an argon laser (488 nm), a laser diode (561 nm), and a helium/neon laser (633 nm) were used [17]. Emission

signals were recorded at 500–550 nm (nucleic acid stained bacteria), 585–625 nm (lectin-specific glycoconjugates), and 650–750 nm (chlorophyll *a*). Samples were examined with water-immersible lenses 20 × 0.5 NA or 63 × 0.9 NA. For each plate, ten images with 63 × (Experiment 1) and ten images with 20 × objective lenses (Experiment 2) were recorded. After microscopy, the plates were transferred to the flume and connected with the control unit again. The next staining and microscopy were done at different locations of the plates.

### 3. Results and Discussion

The fluctuations of pH at the paint surface differed between the four paints in Experiment 1 (Figure 1, red frame). Only small pH changes of about 0.5 in each direction were observed on Paint A. A pH minimum of 5 and a pH maximum of 10 were measured on the surface of Paint B. The pH extremes were always achieved after 4 min at the end of the electrochemical treatment (Figure 1). Paints C and D showed moderate changes in pH between about 6 and 9. The principle functioning of the electrochemical treatment, i.e., the electrochemical generation of pH changes [6–8], was confirmed.

Maximum algal biomass was observed after two weeks of incubation when a well-established biofilm was observed on the control plates. The CLMS images showed dense colonization with diatoms (shown in blue; Figure 2, red frame). A slime matrix of extracellular glycoconjugates (shown in red), which are produced by benthic diatoms [20] and bacteria (shown in green), were also detected. No autofluorescence of the paint was detected in the control without electrochemical treatment. Overall, the control plates showed biofilm images typical for painted surfaces [13]. In comparison to the uncharged control panels, different patterns of surface structure and of fluorescence were observed after electrochemical treatment. The current had modified the paint surface in a way that bound fluorescence dyes to the paint, or the paint showed autofluorescence at the applied wavelength (Figure 2). This was true particularly for Varnishes A–C but not for Varnish D that contained no sol-gel system (Table 1). Thus, the detection of bacteria and EPS was not possible after electrochemical treatment. However, the different patterns of surface structure and fluorescence originating from the paint after electrochemical treatment were not strong enough to obscure autofluorescence of chlorophyll *a*. The number of diatoms was much lower on paints after the electrochemical treatment than on control plates. Counting the algae on treated paints showed the lowest densities on Paints B and D, moderate densities on Paint C, and highest densities on Paint A (Figure 2). This demonstrates a negative relationship between the pH differences and the density of attached algae on the surface of the paint, indicating the effect of the treatment. In the second experiment, the biofilm was characterized by a dense diatom community on the control panel after two weeks (Figure 2, blue frame). Algal numbers were much lower on the electrochemically treated paints, where different patterns of surface structure and fluorescence were observed again. Algal density was equal on plates treated with 20, 40, and 60 min breaks (Figure 2). In contrast, it was significantly higher on plates on which a 99-min break was applied (one-way ANOVA:  $p = 0.024$ ). Therefore, the breaks between electrochemical treatments should not be longer than one hour in order to achieve a maximum antifouling effect. This is important to minimize the electrochemical exposure of the outer layer of the antifouling coating, improving the process stability to achieve the required process times, e.g., at ship hulls.

There is also a need to develop highly conductive varnishes for the second layer of the painted electrode that are not too expensive to achieve electrical conductivities high enough for a homogeneous distribution of current densities on the large immersed surface areas of big ships. The energy demand for the low-voltage electrochemical treatment should not be high. Hypothetically assuming the application of the proposed electrochemical antifouling on MS Gülsün, a large containership (length 383.1 m, width 61.5 m, draught 16.5 m; [21]), to cover an immersed surface area of around 27,000 m<sup>2</sup> (calculated by using the Mumford formula [22]) would need maximum electrical power of around 135 KW (<0.2% of the main engine power of 75,760 kW) for a power density of 5 Wm<sup>-2</sup> on the painted electrodes, corresponding to electrical energy consumption of 3249 KWh per day in continuous operation mode of 894 KWh for Schedule I, and 376 KWh for Schedule III (see Figure 1). Taking into

consideration the investigations of Schultz [1], who calculated an additional need of power by up to 85% to hold the speed of a medium-sized warship (frigate at 15 kn) caused by biofouling, a significant economic benefit can be expected of electrochemical antifouling.

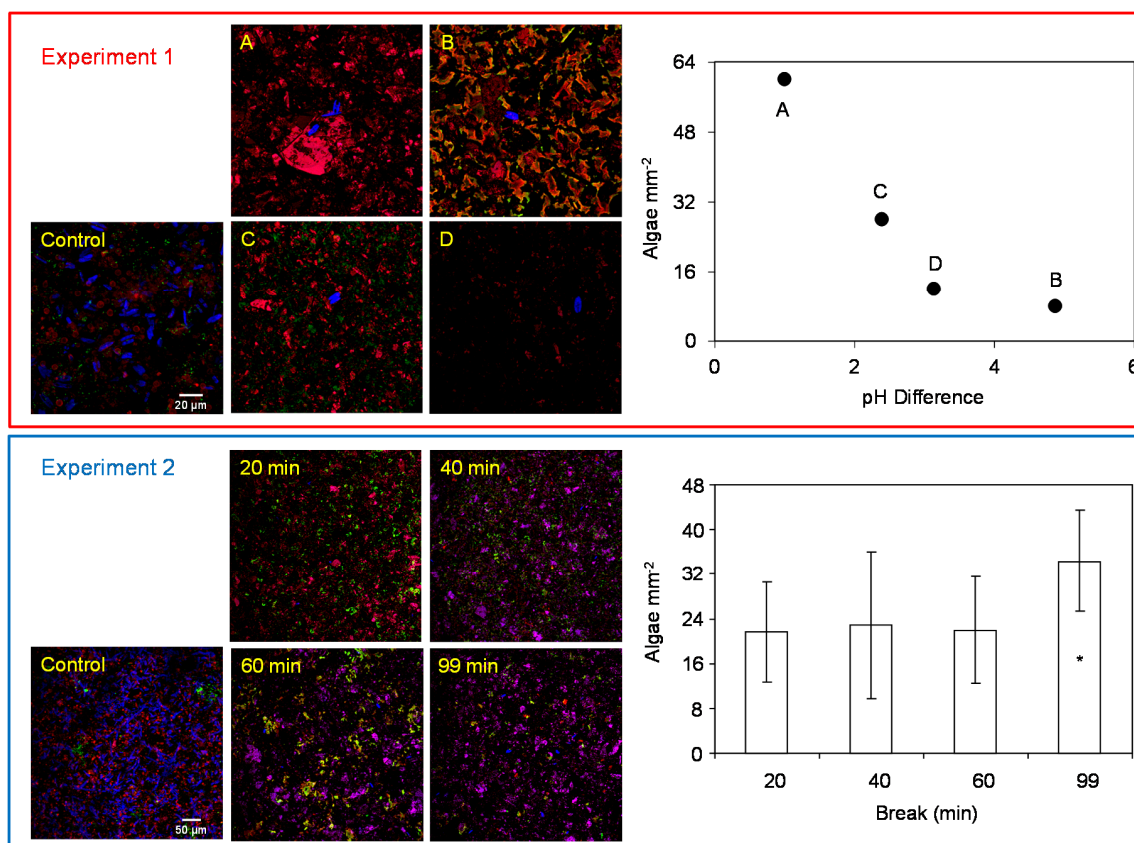


**Figure 2.** Left side: maximum intensity projections of CLSM data sets from biofilms after two weeks incubation: on the control pair of plates with Varnish A without electrolysis current and four paints (Experiment 1; red frame) and on the control and paint with four break times (Experiment 2; blue frame). Colour allocation: blue—autofluorescence of chlorophyll *a*, green—bacteria, red—lectin-specific EPS glycoconjugates. Right side: Algal density on the four paints, A–D (Experiment 1), as a function of the pH difference at the paint surfaces and on Paint A at different break times (Experiment 2; error bars: SD of ten images). The asterisk indicates a significant difference.

#### 4. Conclusions

We established an experimental setup for testing the antifouling capabilities of conductive paints as electrodes. The proposed electrochemical treatment significantly decreases the number of adhered algae in comparison to the control panels. The density of biofilm algae decreased with increasing pH fluctuations during the time schedule of the electrochemical treatment. The result indicates a quantitative relationship between treatment strength and observed effect. Further research should focus on the long-term operational stability of the proposed paints as electrodes for low-current seawater electrolysis. By this means, an optimal electrochemical antifouling and corresponding process stability of the paints may be achieved. The test device presented enables the test of many coatings to find suitable ones for a subsequent application on a larger scale. To enable an application to large surfaces, it is an ongoing challenge to increase the spatial range of electrochemical treatment by highly conductive paints and to prevent leakage of energy by damaged cover coatings. Future investigations should be performed to test conductive paints on larger plates in the sea under field conditions and, in the next step, on the hull of real ships.

**Author Contributions:** Conceptualization, N.K. and T.R.N.; preparation of coatings, U.S., C.M., and G.W.; flume experiment, N.K.; microscopy, T.R.N.; writing—original draft preparation, N.K.; writing—review and editing, U.S. and T.R.N.; project administration, N.K. and T.R.N.; funding acquisition, T.R.N. All authors have read and agreed to the published version of the manuscript.

**Funding:** This paper was promoted by the German Federal Ministry of Economy and Technology (IN0708).

**Acknowledgments:** We thank Ute Kuhlicke for her excellent support in laser microscopy, Birte Matthiessen for providing algal cultures, Stefan Sandrock for useful tips regarding electrochemical treatment and pH measurement, and Barbara Zippel for fruitful discussions within the project. Lars Teichmann and Daniel Goll from the company LAGOTEC constructed the electronic control unit.

**Conflicts of Interest:** The authors declare no conflict of interest. The funders had no role in the design of the study; in the collection, analyses, or interpretation of data; in the writing of the manuscript, or in the decision to publish the results.

## References

- Schultz, M.P. Effect of coating roughness and biofouling on ship resistance and powering. *Biofouling* **2007**, *23*, 331–341. [[CrossRef](#)] [[PubMed](#)]
- Dafforn, K.A.; Lewis, J.A.; Johnston, E. Antifouling strategies: History and regulation, ecological impacts and mitigation. *Mar. Pollut. Bull.* **2011**, *62*, 453–465. [[CrossRef](#)] [[PubMed](#)]
- Yebra, D.M.; Kiil, S.; Dam-Johansen, K. Antifouling technology—past, present and future steps towards efficient and environmentally friendly antifouling coatings. *Progr. Org. Coat.* **2004**, *50*, 75–104. [[CrossRef](#)]
- Genzer, J.; Efimenko, K. Recent development of superhydrophobic surfaces and their relevance to marine fouling: A review. *Biofouling* **2006**, *22*, 339–360. [[CrossRef](#)] [[PubMed](#)]
- Little, B.; Lee, J.; Ray, R. A review on ‘green’ strategies to prevent or mitigate microbiologically influenced corrosion. *Biofouling* **2007**, *23*, 87–97. [[CrossRef](#)] [[PubMed](#)]
- Sandrock, S.; Scharf, E.-M.; Schubert, H. Methods for Influencing the pH Value on Surfaces of Solids in Liquid Media. German Patent DE 41 09 198, 18 March 1991. Available online: <https://patents.google.com/patent/DE4109198A1/de?oq=DE+4109198> (accessed on 20 May 2020).
- Sandrock, S.; Scharf, E.-M.; Schubert, H. Methods for the Prevention of Growth on Submerged Surfaces by Sporadic, Controlled Changes of Their Physical Properties. German Patent DE 41 09 197, 18 March 1991. Available online: <https://patents.google.com/patent/DE4109197A1/de?oq=DE+4109197> (accessed on 20 May 2020).
- Sandrock, S.; Scharf, E.-M.; Reiter, K.; Franz, A.; Günther, E. Coating of Surfaces Entering into Contact with a Liquid in Order to Prevent Biological Vegetation. European Patent EP 1570010 B1, 20 March 2002. Available online: <https://patents.google.com/patent/EP1570010B1/de?oq=EP+1570010+> (accessed on 21 May 2020).
- Huang, Y.; Saito, K.; Usami, M. A study on antifouling technique through seawater electrolyzing reaction on ship hull surface. *J. Int. Dev. Coop.* **2003**, *9*, 23–28.
- Huang, J.-R.; Lin, W.-T.; Huang, R.; Wu, J.-K. Antifouling properties of conductive rubber coatings used for fishing nets. *J. Mar. Sci. Technol.* **2009**, *17*, 173–179.
- Debiemme-Chouvy, C.; Hua, Y.; Hui, F.; Duval, J.-L.; Cachet, H. Electrochemical treatments using tin oxide anode to prevent biofouling. *Electrochim. Acta* **2011**, *56*, 10364–10370. [[CrossRef](#)]
- Bunn, M.; Yokochi, A.; von Jouanne, A. Electrochemical antifouling technology for replacement of heavy metal and organic biocides in marine hydrokinetic energy generation. In Proceedings of the 2014 IEEE Conference on Technologies for Sustainability (SusTech), Portland, OR, USA, 24–26 July 2014; pp. 35–40.
- Kamjunke, N.; Spohn, U.; Fütting, M.; Wagner, G.; Scharf, E.-M.; Sandrock, S.; Zippel, B. Use of confocal laser scanning microscopy for biofilm investigation on paints under field conditions. *Int. Biodet. Biodegr.* **2012**, *69*, 17–22. [[CrossRef](#)]
- Casse, F.; Swain, G.W. The development of microfouling on four commercial antifouling coatings under static and dynamic immersion. *Int. Biodet. Biodegr.* **2006**, *57*, 179–185. [[CrossRef](#)]
- Molino, P.J.; Wetherbee, R. The biology of biofouling diatoms and their role in the development of microbial slimes. *Biofouling* **2008**, *24*, 365–379. [[CrossRef](#)] [[PubMed](#)]
- Molino, P.J.; Campbell, E.; Wetherbee, R. Development of the initial microfouling layer on antifouling and fouling-release surfaces in temperate and tropical Australia. *Biofouling* **2009**, *25*, 685–694. [[CrossRef](#)] [[PubMed](#)]

17. Neu, T.R.; Woelfl, S.; Lawrence, J.R. Three-dimensional differentiation of photo-autotrophic biofilm constituents by multi-channel laser scanning microscopy (single-photon and two-photon excitation). *J. Microbiol. Meth.* **2004**, *56*, 161–172. [[CrossRef](#)] [[PubMed](#)]
18. Fay, F.; Horel, G.; Linossier, I.; Vallee-Rehel, K. Effect of biocidal coatings on microfouling: In vitro and in situ results. *Progr. Org. Coat.* **2018**, *114*, 162–172. [[CrossRef](#)]
19. Neu, T.R.; Swerhone, G.D.W.; Lawrence, J.R. Assessment of lectin-binding analysis for in situ detection of glycoconjugates in biofilm systems. *Microbiology* **2001**, *147*, 299–313. [[CrossRef](#)] [[PubMed](#)]
20. Bhosle, N.B.; Evans, L.V.; Edyvean, R.G.J. Carbohydrate production by *Amphora coffeaeformis*, a marine fouling diatom. *Biofouling* **1993**, *7*, 81–91. [[CrossRef](#)]
21. MSC Shipping Company. *MSC Gülsün*; MSC Shipping Company: Geneva, Switzerland, 2019. Available online: [https://de.wikipedia.org/wiki/MS\\_C\\_Megamax-24](https://de.wikipedia.org/wiki/MS_C_Megamax-24) (accessed on 26 May 2020).
22. MAN Energy Solutions. *Basic Principles of Ship Propulsion*; Chapter 1; MAN Energy Solutions: Copenhagen, Denmark, 2018; pp. 9–11. Available online: [https://marine.man-es.com/docs/librariesprovider6/test/5510-0004-04\\_18-1021-basic-principles-of-ship-propulsion\\_web\\_links.pdf?sfvrsn=12a35ba2\\_30](https://marine.man-es.com/docs/librariesprovider6/test/5510-0004-04_18-1021-basic-principles-of-ship-propulsion_web_links.pdf?sfvrsn=12a35ba2_30) (accessed on 26 May 2020).



© 2020 by the authors. Licensee MDPI, Basel, Switzerland. This article is an open access article distributed under the terms and conditions of the Creative Commons Attribution (CC BY) license (<http://creativecommons.org/licenses/by/4.0/>).